

# MAPPING LOCAL CLIMATE ZONES WITH A VECTOR-BASED GIS METHOD

*E. LELOVICS<sup>1</sup>, T. GÁL<sup>2</sup>, J. UNGER<sup>3</sup>*

## **ABSTRACT.** – Mapping Local Climate Zones with a vector-based GIS method.

In this study we determined Local Climate Zones in a South-Hungarian city, using vector-based and raster-based databases. We calculated seven of the originally proposed ten physical (geometric, surface cover and radiative) properties for areas which are based on the mobile temperature measurement campaigns earlier carried out in this city.

As input data we applied 3D building database (earlier created with photogrammetric methods), 2D road database, topographic map, aerial photographs, remotely sensed reflectance information from RapidEye satellite image and our local knowledge about the area. The values of the properties were calculated by GIS methods developed for this purpose.

We derived for the examined areas and applied for classification sky view factor, mean building height, terrain roughness class, building surface fraction, pervious surface fraction, impervious surface fraction and albedo.

Six built and one land cover LCZ classes could be detected with this method on our study area. From each class one circle area was selected, which is representative for that class. Their thermal reactions were examined with the application of mobile temperature measurement dataset. The comparison was made in cases, when the weather was clear and calm and the surface was dry. We found that compact built-in types have more temperature surplus than open ones, and midrise types also have more than lowrise ones. According to our primary results, these categories provide a useful opportunity for intra- and inter-urban comparisons.

**Keywords:** urban heat island, Local Climate Zones, GIS method, Szeged, Hungary.

## **1. INTRODUCTION**

Due to the anthropogenic activity, a local climate develops in the built-up area. This so-called urban climate is the result of construction buildings and impervious surfaces, emission of heat, moisture and air pollution related to human activities. Most obvious modification among meteorological variables is shown by the near-surface (for example screen-height) air temperature (Oke, 1987). This urban-rural temperature anomaly is commonly referred to as the urban heat island (UHI) and its magnitude is the UHI intensity ( $\Delta T_{u-r}$ ).

---

<sup>1</sup> University of Szeged, Department of Climatology and Landscape Ecology, 6722 Egyetem u. 2., Szeged, Hungary, e-mail: lelovics@geo.u-szeged.hu

<sup>2</sup> University of Szeged, Department of Climatology and Landscape Ecology, 6722 Egyetem u. 2., Szeged, Hungary, e-mail: tgal@geo.u-szeged.hu

<sup>3</sup> University of Szeged, Department of Climatology and Landscape Ecology, 6722 Egyetem u. 2., Szeged, Hungary, e-mail: unger@geo.u-szeged.hu

Stewart and Oke (2012) developed a climate-based classification system for describing the local physical conditions around the temperature measuring field sites (e.g. Auer, 1978; Ellefsen, 1990/91; Oke, 2004). The elements of this system are the “local climate zones” (LCZ).

Because of the complexity of the urban terrain the monitoring of the representative intra-urban thermal features is a difficult task (Oke, 2004). This kind of classification can be useful for describing the examined area. In the case of an already existing network (e.g. Schroeder et al., 2010) it may be required to characterize the relatively wider environment around the measuring sites. In the case of a planned station network (e.g. Unger et al., 2011) the most important questions are what built and land cover LCZ types can be distinguished in a given urban area, how precisely they can be delimited, how many they are, and whether their extension is large enough to install a station somewhere in the middle of the area (representing the thermal conditions of this LCZ).

The aims of our study are: to determine the LCZ types in Szeged which are representative for the urbanized area of the city using seven geometric, surface cover and radiative properties from the ten ones listed by Stewart and Oke (2012), to develop GIS methods in order to calculate these seven property values for any part of the study area and to compare the thermal reactions of the selected LCZ areas based on the earlier temperature measurement campaigns carried out in this city.

## 2. STUDY AREA, DATABASE AND METHOD

### 2.1. Study area, temperature measurements

Szeged (N 46°, E 20°, 79 m a.s.l.) is located in the south-eastern part of Hungary (Fig. 1a and 1b). It has 160,000 inhabitants and 281 km<sup>2</sup> administration area. Its environment is a flat terrain with climatic region Cf (temperate warm climate with a rather uniform annual distribution of precipitation) according to Köppen’s climatic classes. Annual mean temperature is 10.4 °C, precipitation is 497 mm (Unger et al., 2001). Our study area contains urban and suburban parts of Szeged, which is covered with 103 cells, sized 500 × 500 m and 4 additional detached cells at the western side, representing the non built-up area.

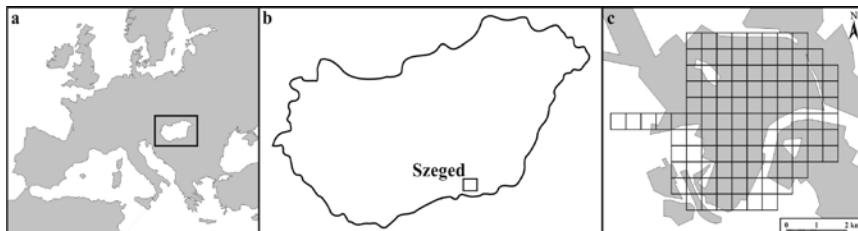


**Fig. 1. (a) Location of the Szeged in Europe, (b) in Hungary and (c) the grid network of the study area (gray – urbanized area).**

Temperature measurements were taken by cars during a one-year period in 2002/2003 several times. Sensors were mounted at 1.45 m a.g.l., using radiation screen. Data were collected every 10 s, so at a car speed of 20-30 km h<sup>-1</sup> the distance between measuring points was 55-83 m. The logged values at forced stops were omitted. 15-20 measurements in each grid were averaged and considered as belong to the cell center. Return routes were taken to make time-based corrections to a reference time, 4 hours after sunset (Unger, 2004, Balázs et al., 2009).

We selected four nights when the weather was clear and calm in the preceding days too, the ground was relatively dry, and the trees had foliage, thus during these nights the weather conditions promoted the surface influence on the thermal conditions in the near-surface air layer. As the best conditions for UHI development prevail in summer and early autumn in this region (WMO, 1996) two nights were selected in summer (15 July 2002, 21 August 2002), one in autumn (18 September 2002), and additionally one in spring (25 March 2003).

## 2.2. Local Climate Zones categories

The necessity and ideas of the development of “local climate zones” classification system and its structure are presented and discussed in details by Stewart and Oke (2012). They are local regions having uniform surface structure and human activity. When the circumstances promote microclimates to differ (for example on calm, clear nights, when radiation and heat conduction processes can prevail without remarkable mixing and advection), these regions have a characteristic temperature regime, which is originated from similar microenvironments of these zones. Among these categories are 10 built types and 7 land cover types, and additionally they have 4 temporal properties (Table 1).

**Table 1. Local Climate Zones categories (after Stewart and Oke, 2012)**

Built categories	Land cover categories	Variable land cover properties
LCZ 1 – Compact high-rise	LCZ A – Dense trees	b – bare trees
LCZ 2 – Compact midrise	LCZ B – Scattered trees	s – snow cover
LCZ 3 – Compact low-rise	LCZ C – Bush, scrub	d – dry ground
LCZ 4 – Open high-rise	LCZ D – Low plants	w – wet ground
LCZ 5 – Open midrise	LCZ E – Bare rock / paved	
LCZ 6 – Open low-rise	LCZ F – Bare soil / sand	
LCZ 7 – Lightweight low-rise	LCZ G – Water	
LCZ 8 – Large low-rise		
LCZ 9 – Sparsely built		
LCZ 10 – Heavy industry		

These categories can be characterized with their typical physical properties. Among these parameters there are geometric, surface cover, radiative, thermal and metabolic characteristics. Stewart and Oke (2012) give the typical values of sky view factor (SVF), aspect ratio (HW), building surface fraction (BSF), pervious surface fraction (PSF), impervious surface fraction (ISF), height of

roughness elements (HRE), terrain roughness class (TRC), surface admittance (SA), albedo (ALB), anthropogenic heat emission (AHE) for these classes.

### **2.3. Calculation of physical properties**

We determined 7 of the earlier enumerated physical properties with GIS methods, from vector-based and raster-based databases, using mainly remote-sensed information. These calculations were made for circle areas with center at the center of grids used in temperature measurements and with 250 m radius. This size is necessary as the upwind fetch of typically 200-500 m is required for air at screen-height to become fully adjusted to the underlying, relatively homogeneous surface (Stewart and Oke, 2012).

SVF was averaged from a SVF database with 5 m horizontal resolution, originated from our earlier studies (Gál et al., 2009). It was calculated using the building 3D database of Szeged, which contains building footprint areas as polygons, and a height value for each building, measured with photogrammetrical methods (Unger, 2006). It was calculated with a vector-based method, where buildings were regarded with flat roof, and the effect of the vegetation was neglected (Gál et al., 2009).

BSF is the fraction of summarized area of buildings inside the circle. Its input is the 3D building database of Szeged. In the case of buildings on the border of the circle only the area of intersecting part was taken into account.

PSF was basically determined from NDVI calculated from atmospherically corrected RapidEye satellite image, regarded as pervious area where NDVI is above 0.3. Horizontal resolution of this image is 5.16 m. As a first correction we used Corine Land Cover (CLC) database (Bossard et al., 2000) to locate agricultural areas, because after harvest the amount of plants is almost zero, thus their NDVI is small. Second correction was made with the shape of water bodies digitized from a topographic map, because water has NDVI values very similar to values of some building materials. Last we used the road database to locate roads, which are in urban environment usually under tree cover, and which don't appear in CLC database.

ISF was calculated from BSF and PSF, using this formula:  $ISF = 1 - (BSF + PSF)$ .

HRE was calculated from the 3D building database of Szeged. Height of buildings (and building parts) were averaged for each examined circle area, weighted with their footprint area.

TRC was determined with the application of the Davenport roughness classification method (Davenport et al., 2000). Circle areas were classified with visual interpretation of aerial photographs, topographic maps and the building database.

ALB was calculated from the atmospherical corrected values of the 5 band RapidEye satellite image. Broadband albedo was calculated after Starks et al. (1991) as average of reflectance values, weighted with radiation (ASTM, 2012) integrated within the spectral range belongs to a channel.

### 3. RESULTS

We calculated physical properties for each circle area, to apply them in the classification. Our only information about the vegetation is NDVI, that is not enough to make differences between land cover type categories (for example dense trees, scattered trees, bush or low plants), thus our aim was to identify urban categories. It is known, that in Szeged, the following categories don't exist: close high-rise (LCZ 1), open high-rise (LCZ 4), lightweight low-rise (LCZ 7) and heavy industry (LCZ 10). For the remaining six built-in types we have found representative cells. Our westernmost cell was regarded LCZ D (low plants) because it consists of agricultural fields with low plants without trees, and a few small houses. For examining the temperature differences, we selected one representative cell from each category. Fig. 2 shows aerial photographs of these circle areas, fig. 3 shows them on the grid map of the study area.

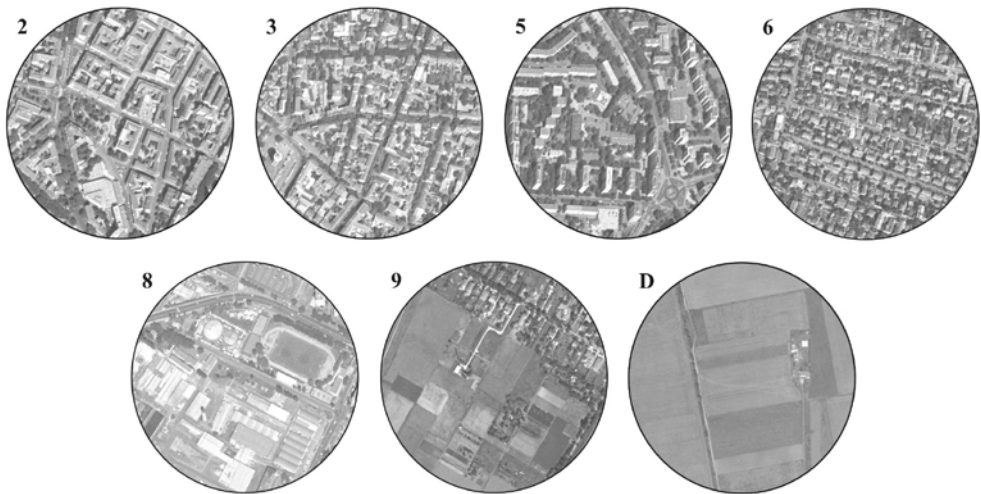


**Fig. 2. Aerial photographs of the circle areas with their designations representing the LCZ types occurring in Szeged**

These cells were selected mainly according to their calculated physical properties and their originally proposed values (shown in table 2), nevertheless there are some deviations (marked with italics in table 2).

The physical parameters of the selected cells relative to the values given by Stewart and Oke (2012) are shown in table 2, and deviations between them are described here shortly cell by cell:

- LCZ 3 (compact lowrise): Its BSF is under the lower limit, thus its SVF is larger than the given upper limit. It could be LCZ 6 (open lowrise), but its PSF is under 0.18, which is typical to LCZ 3, and albedo also justifies this selection.

- LCZ 5 (open midrise): This area is more vegetated than the “ideal” open midrise, thus its BSF is lower, PSF is higher than the given values, but regarding its HRE (15.4 m) and the aerial photograph it must be one of the midrise categories.
- LCZ 8 (large lowrise): Properties of this cell are influenced by the sport field – its BSF is low and its PSF is high. ISF is also higher than the upper limit, but large lowrise is a category where extended asphalt surfaces are justifiable. According to its parameter values it could also be LCZ 6 (open lowrise), in this case it would have more outlier parameters, but their deviation would be smaller. However, as the picture in Figure 3 shows, it is a typical warehouse area with factory buildings, so it is classified as LCZ 8.
- LCZ 9 (sparsely built): Its BSF is under the lower limit and ISF is higher than the upper limit. It could be even one of the land cover LCZ types (for example LCZ D), but aerial photograph justifies selection of LCZ 9, and the mobile temperature measurement route was on the more built-in part of this cell.

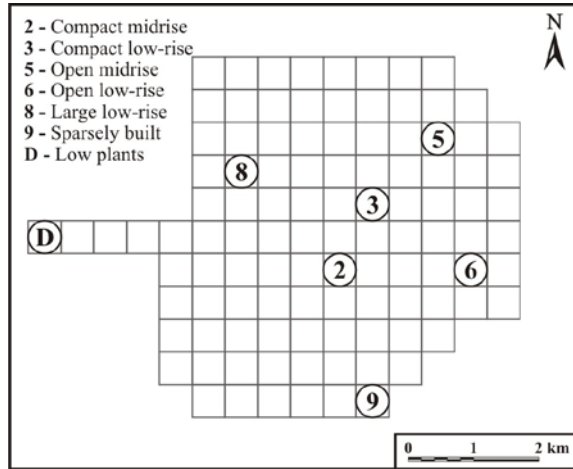


**Fig. 3. Selected areas on the grid map of Szeged**

**Table 2. Ranges of the properties for LCZ types (Stewart and Oke, 2012) compared to the values of the representative areas in Szeged (italic values deviate from the given ranges)**

LCZ category	Properties						
	SVF	BSF	ISF	PSF	HRE [m]	TRC	ALB
LCZ 2 (CM)	0.30–0.60	0.40–0.70	0.30–0.50	0.00–0.20	10–25	6–7	0.10–0.20
	0.59	0.45	0.44	0.11	13.6	7	0.15
LCZ 3 (CL)	0.20–0.60	0.40–0.70	0.20–0.50	0.00–0.30	3–10	6	0.10–0.20
	0.68	0.31	0.50	0.18	7.9	6	0.14
LCZ 5 (OM)	0.50–0.80	0.20–0.40	0.30–0.50	0.20–0.40	10–25	5–6	0.12–0.25
	0.74	0.16	0.42	0.42	15.4	6	0.12
LCZ 6 (OL)	0.60–0.90	0.20–0.40	0.20–0.50	0.30–0.60	3–10	5–6	0.12–0.25
	0.83	0.20	0.45	0.34	5.4	6	0.16
LCZ 8 (LL)	0.70–1.00	0.30–0.50	0.40–0.50	0.00–0.20	3–10	5	0.15–0.25
	0.92	0.15	0.60	0.25	6.6	5	0.16
LCZ 9 (SB)	0.80–1.00	0.10–0.20	0.00–0.20	0.60–0.80	3–10	5–6	0.12–0.20
	0.99	0.03	0.22	0.75	5.0	4	0.17
LCZ D (LP)	0.90–1.00	0.00–0.10	0.00–0.10	0.90–1.00	0–1	3–4	0.15–0.25
	0.99	0.00	0.00	1.00	0.0	3	0.15

For these selected cells temperature anomaly values are shown in fig. 4, where LCZ D cell plays the role of the reference. As it is expected, compact built-in types have more temperature surplus than open ones, and midrise types also have more than lowrise ones. In average temperature of the LCZ 2 compact midrise cell exceeds temperature of the LCZ D low plant one with 4.2 °C. Large lowrise area also has a relatively large temperature anomaly.

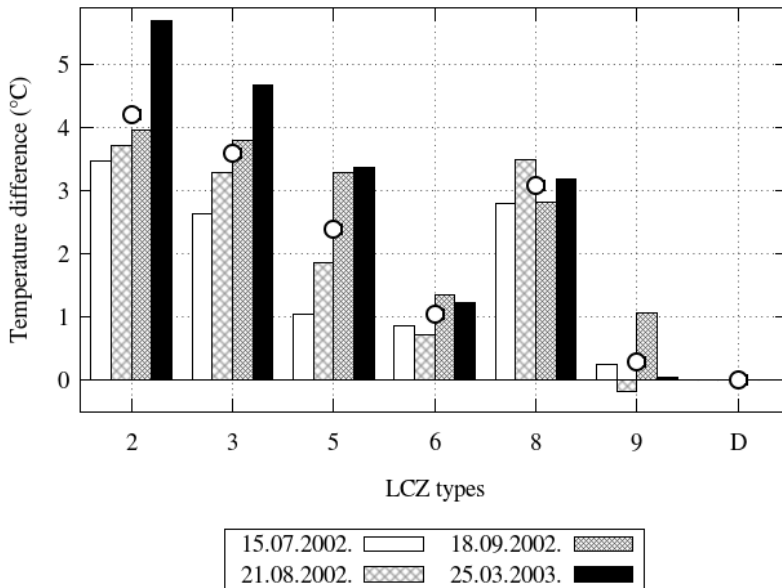


**Fig. 4.** *Temperature differences between selected cells and cell representing LCZ D (4 nights and their average)*

#### 4. CONCLUSIONS

In this study we determined the LCZ types in Szeged which are representative for the urbanized area of the city using seven geometric, surface cover and radiative properties from the ten ones listed by Stewart and Oke (2012) and compared their thermal reactions based on the earlier temperature measurement campaigns carried out in this city. As a result, six built and one land cover LCZ types were distinguished in the studied urban area. We found that compact built-in types have more temperature surplus than open ones, and midrise types also have more than lowrise ones.

**ACKNOWLEDGEMENT.** – The study was supported by the Hungarian Scientific Research Fund (OTKA PD-100352). The authors’ thanks are due to László Mucsi (University of Szeged) for providing the RapidEye satellite image.

## REFERENCES

1. ASTM (2012), American Society for Testing and Materials Reference Solar Spectral Irradiance: Air Mass 1.5 <http://rredc.nrel.gov/solar/spectra/am1.5/> accessed on January, 25, 2013.
2. Auer, A.H. (1978) Correlation of land use and cover with meteorological anomalies. *Journal of Applied Meteorology* 17: 636-643.
3. Balázs, B., Unger, J., Gál, T., Sümeghy, Z., Geiger, J. Szegedi, S. (2009), *Simulation of the mean urban heat island using 2D surface parameters: empirical modeling, verification and extension*. Meteorological Application 16, 275–287.
4. Bossard, M., Feranec, J., Otahel, J. (2000), *CORINE land cover technical guide – Addendum 2000*. Technical report No 40. European Environment Agency, Copenhagen, Denmark.
5. Davenport, A.G., Grimmond, C.S.B., Oke, T.R., Wieringa, J. (2000), *Estimating the roughness of cities and sheltered country*. 12th AMS Conference on Applied Climatology (Asheville), 96-99.
6. Ellefsen, R. (1990/91) Mapping and measuring buildings in the canopy boundary layer in ten U.S. cities. *Energy and Buildings* 15-16: 1025-1049.
7. Gál, T., Lindberg, F., Unger, J. (2009), *Computing continuous sky view factors using 3D urban raster and vector databases: comparison and application to urban climate*. Theoretical and Applied Climatology 95, 111–123.
8. Oke T.R. (1987) *Boundary Layer Climates*. (2nd ed.) Routledge, London-New York.
9. Oke T.R. (2004) *Initial guidance to obtain representative meteorological observation sites*. WMO/TD No. 1250, Geneva, Switzerland.
10. Schroeder, A. J., Basara, J. B. and Illston, B. G. (2010) Challenges associated with classifying urban meteorological stations: The Oklahoma City Micronet example. *Open Atmospheric Science Journal* 4: 88-100.
11. Starks, P.J., Norman, J.M., Blad, B.L., Walter-Shea, E.A., Walthall, C.L. (1991), *Estimation of Shortwave Hemispherical Reflectance (Albedo) from Bidirectionally Reflected Radiance Data*. Remote Sensing of Environment 38, 123–134.
12. Stewart, I.D., Oke, T.R. (2012), *Local Climate Zones for urban temperature studies*. Bulletin of the American Meteorological Society 93, 1879–1900.
13. Unger, J. (2004), *Intra-urban relationship between surface geometry and urban heat island: review and new approach*. Climate Research 27, 253–264.
14. Unger, J. (2006), *Modelling of the annual mean maximum urban heat island using 2D and 3D surface parameters*. Climate Research 30, 215–226.
15. Unger, J., Sümeghy, Z., Gulyás, Á., Bottyán, Z. and Mucsi, L. (2001) *Land-use and meteorological aspects of the urban heat island*. Meteorological Applications 8, 189-194.
16. Unger, J., Savic, S. and Gál, T. (2011) Modelling of the annual mean urban heat island pattern for planning of representative urban climate station network. *Advances in Meteorology* 2011: ID 398613, 9p.
17. WMO, (1996), *Climatological Normals (CLINO) for the period 1961–1990*. WMO/OMM-No. 847. Secretariat of the World Meteorological Organization, Geneva, Switzerland.